

Hydrostatic Pivoted Pad Bearing for Oil-Free Turbomachinery

Lyn M. Greenhill

Valerie J. Lease

DynaTech Engineering, Inc.

Roseville, CA, 95661 USA

ABSTRACT

To replace traditional rolling element bearings and eliminate liquid lubricants used in small gas turbine engines, a unique bearing configuration has been developed – the Hydrostatic Pivoted Pad Bearing, or HyPad[®]. This patent-pending concept consists of several pivoting pads, through which a number of holes are placed to create a hydrostatic gas film. During operation, the gas film, supplied from a small amount of compressor bleed air, more than adequately supports normal loads, with contact between the rotor and bearing only during start/stop and high load conditions, such as maneuvers. To permit limited contact and provide wear resistance, the pads are constructed from a proprietary self-lubricating material. The combination of the hydrostatic assist with self lubricated pivoting pads offers desirable rotor dynamic properties, including high stiffness, reasonable damping, and very low cross coupling, resulting in excellent stability characteristics. The feasibility of the HyPad was demonstrated both analytically and by actual testing in a gas bearing rig, with superb performance obtained from the prototype hardware to a surface speed over 2.5 million DN, the practical limit for most rolling element bearings. Results from the analysis and testing are presented in this paper, to demonstrate the operating characteristics and potential of this unique bearing concept.

Keywords: Oil-Free Bearing Hydrostatic Gas Film Pivoted Pad Rotor Dynamics Testing

INTRODUCTION

A very attractive alternative to the use of rolling element bearings in gas turbines are air film bearings, which eliminate the liquid lubrication system and represent a significant breakthrough in technology. Development efforts with air film bearings in gas turbines have been conducted for perhaps 30 years. Most of the oil-free concepts have featured foil bearings [1]. Although these bearings offer clear advantages to rolling element bearings, such as higher temperatures, low maintenance, and greater shaft speeds, application to turbomachinery other than small auxiliary equipment has been limited due to an inherent lack of load capacity and minimal amounts of damping. Although gains have been made in unit loading, the damping problem severely limits application to supercritical rotor systems, which are essential for light, high power density gas turbines. A lack of predictability has also been a key limiting factor, since current analysis techniques are unable to accurately determine performance, resulting in extensive empirical development for each application. The analytical difficulties are largely due to the complex interaction between the hydrodynamic gas film and the elastic foils. Because the performance parameters are not well quantified, each bearing is essentially a custom piece of hardware, with resulting variability in supposedly identical units, and limited scalability.

In contrast, the HyPad air film bearing described in this paper is a combination of several technologies designed primarily to address the shortcomings of hydrodynamic bearings, such as foils. The pivoting pads are fabricated from a self-lubricating material, with the air film created hydrostatically. Unlike the hydrodynamic film created in foil bearings, the hydrostatic support offers substantially more load capacity, supplied from a small amount of pressurized air from the compressor. Design of the hydrostatic gas film is a relatively straightforward analytical procedure, with good agreement obtained with test results.

The multiple pad configuration of the HyPad, shown in Figure 1, was chosen to address dynamic properties, ease of manufacture, and the small clearances required with air bearings. With oil film bearings, the optimum configuration from a rotor stability standpoint are tilting pads, which essentially eliminate the cross-coupled stiffness and damping terms. The HyPad applies this concept directly, focusing on the direct dynamic coefficients. Individual pads also permit easier machining of the hydrostatic passages, and allow for precise adjustment of build clearance. With gas films, the gap between the rotor and stator is usually only a few thousandths of an inch, so accurate control of clearance is very important for reliable and predictable operation.

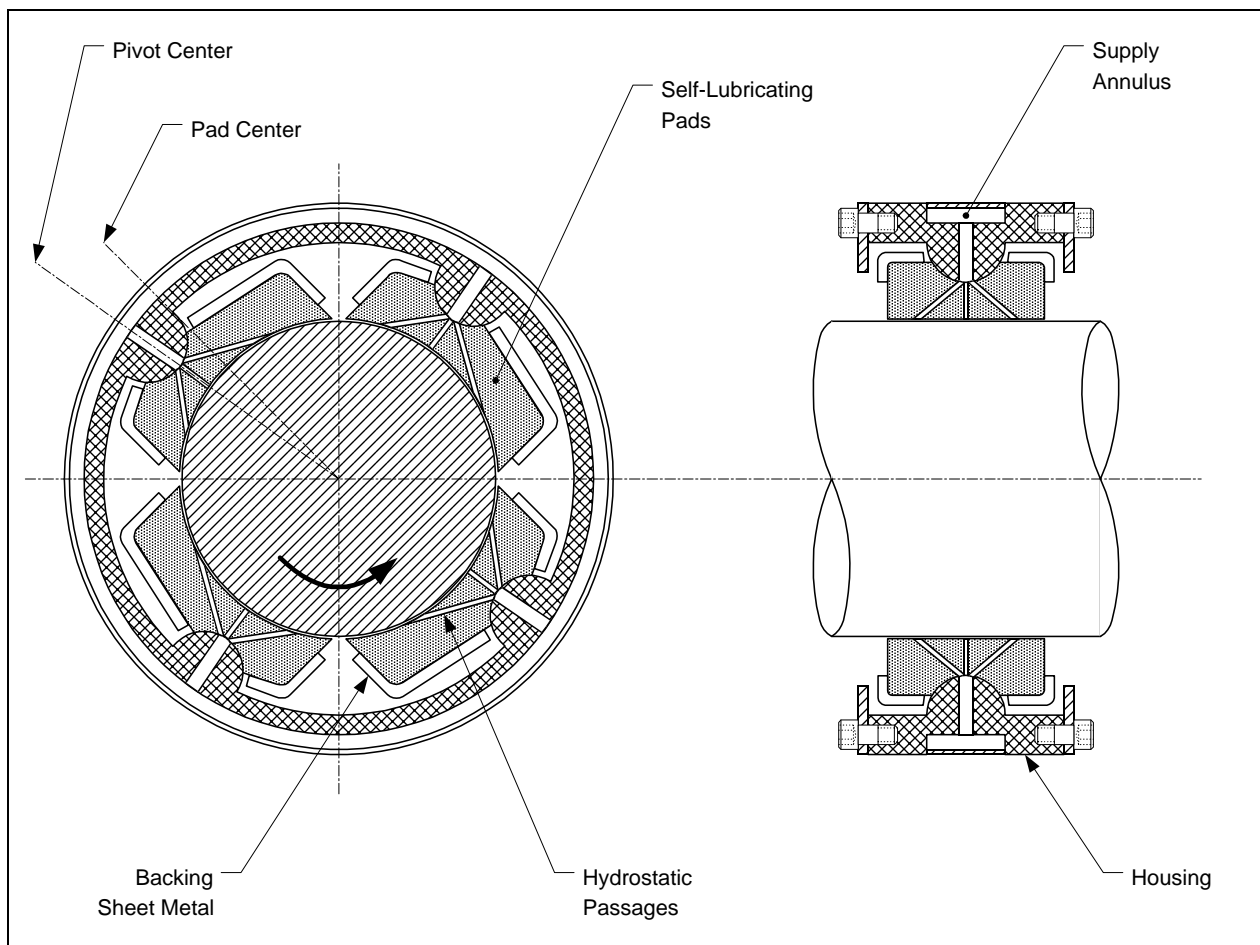


Figure 1. HyPad design configuration

In operation, normal loads are supported by the HyPad gas film, which can have a load capacity several times what is required. During situations where extreme loads are applied, such as with maneuver transients or excessive unbalance (blade loss), the rotor can ride directly on the HyPad surface for a limited amount of time, since the pad is self-lubricating. This bilinear load-deflection characteristic can be tailored to provide optimum dynamic properties in both operating regimes. This is a sharp contrast to the behavior of foil bearings, which cannot tolerate excessive load without serious damage, including seizure.

The hydrostatic air supply is channeled to the pad pivot, which connects with a number of orifices to create the hydrostatic pressure drop and gas film. The air passages are angled in various directions, however, the net flow can be introduced to *oppose* shaft rotation, which can significantly improve damping. There are no pockets on the bearing surface, as is common with fluids, just a small conical exit, to eliminate potential pneumatic instability. The pad pivot is spherical, to allow articulation in the radial and axial directions, while providing an anti-rotation restraint. The pivot point on the pad is shown slightly biased in the direction of rotation, for inherent clearance adjustment and load sharing capability. In addition, the bearing is preloaded, in which the curvature of the pads is slightly larger than the shaft, to improve load distribution and rotor dynamic stability. A metallic backing is used on the outside of the pads for structural support. Although there are many intricate design features in each pad, the ability to work on each pad as a separate article permits such detail to be easily obtained in manufacture. Individual pads should also be easy to replace in the field should maintenance be required.

Work on the HyPad to date has validated the concept as a replacement for oil-lubricated rolling element bearings. The following achievements have been attained:

- Three different analytical techniques were used to design prototype hardware, ranging from hand calculations to computational fluid dynamics. All three methods were in good agreement.
- Prototype hardware was evaluated in a high-speed gas bearing rig at Texas A & M University. A speed of nearly 90,000 rpm was attained, representing a bearing DN over 2.5 million. Stability was excellent, with no significant subsynchronous vibration observed during operation at any speed.
- Results from testing have been used to correlate analytical predictions, with adjustments indicated to match test data. In particular, the amount of damping obtained in testing was significantly greater than actually predicted.

The feasibility tests demonstrate that the concept has significant potential and applicability. With the added advantage of a much more direct and simpler analysis approach, the HyPad is clearly a strong alternative to conventional hydrodynamic air bearings for use with moderate size gas turbine engines. A description of the analytical techniques used to design the bearing will be presented, along with results and correlations obtained from testing.

DESIGN ANALYSIS

A series of flow analyses were performed on the hydrostatic geometric features of the HyPad to establish a reasonable prototype test configuration. Because the HyPad represents a departure from available analysis methodology, three different approaches were used:

1. A closed form calculation procedure developed by Jorgen Lund for full annular radial gas hydrostatic bearings.
2. An individual pad, laminar, compressible flow Reynolds equation solution developed by Dr. Luis San Andrés from Texas A & M.
3. A computational fluid dynamics (CFD) analysis of a single pad.

Results from the three analysis procedures were relatively consistent and provided a measure of confidence that the HyPad design would perform properly.

Although it was originally intended to optimize the location and number of feed holes through analysis, it became obvious early in the development of the prototype that either 5 or 1 hole(s) per pad were the only reasonable choices, primarily based on manufacturability. Larger hole counts (such as 9) were initially considered, however, for the size of the pads used in the prototype, and also with small gas turbine engines, the physical geometry simply does not permit more than five holes to be machined at the pad pivot center. Using 5 holes (one in the center and four angled) would create a flow pressure distribution that would self-align the pad, so this was selected as the most optimum number. A single, straight through hole is the simplest configuration, but may have lower load capacity.

The most basic analytical method used to design HyPad hardware is a procedure described by Lund [2], based on work originally conducted in the early 1960's. Since this period predates large scale use of computers, all of the analysis consists of closed form equations and plots of flow and stiffness relations. For use in the HyPad analysis, the Lund relationships were mainly used to establish an initial orifice size, to insure that pneumatic hammer would not occur, and to predict stiffness. Unfortunately, the Lund analysis does not provide damping coefficients.

Significant factors in the Lund analysis are inherent compensation factor (δ), feeder hole volume ratio (V_r), and restrictor coefficient (Λ_s). These parameters are defined as:

$$\delta = \frac{a^2}{Cd} \quad (1)$$

$$V_r = \frac{NV_c}{\pi DLC} \quad (2)$$

$$\Lambda_s = \frac{6\mu Na^2 \sqrt{RT}}{P_s C^3 \sqrt{1 + \delta^2}} \quad (3)$$

where a is the radius of the flow orifice, C the radial clearance, d the exit hole diameter, N the number of feed holes, V_c the exit hole volume (pocket volume), D is shaft diameter, L is bearing length, μ is gas viscosity, R is gas constant, T is gas temperature, and P_s is supply pressure. The three parameters in equations (1) through (3) establish the flow and stiffness of the bearing, with the feeder hole volume ratio significant from a pneumatic hammer standpoint. In all the configurations considered, V_r was always kept near 0.05, the recommended value. For optimum stiffness, the product of the restrictor coefficient Λ_s and the length to diameter ratio (L/D) should be between 0.5 and 0.7, and if less than 0.3, the feed holes are choked.

The Reynolds equation solution developed by Dr. San Andrés is a computational procedure that analyzes the fluid flow regime only on the pad surface. For a given distribution of feed holes, the pressure profile is predicted, including the effects of speed. This solution is based on the laminar flow of a compressible fluid within the film lands of a bearing pad, described by:

$$-\frac{\partial}{\partial x} \left\{ \frac{\rho h^3}{12\mu} \frac{\partial P}{\partial x} \right\} + \frac{\partial}{\partial z} \left\{ \frac{\rho h^3}{12\mu} \frac{\partial P}{\partial z} \right\} + \frac{\partial}{\partial t} \{ \rho h \} + \frac{1}{2} \frac{\partial}{\partial x} \{ \rho h U \} = m_o \quad (4)$$

where P is the fluid pressure, h is the film thickness, and (ρ, μ) are the fluid density and viscosity, respectively. The rotor surface speed is $U = \Omega D/2$ and m_o is the mass flow per unit area at the location of a feed orifice. The pressure at the bearing sides equals the ambient value, P_a .

For an ideal gas, the density is proportional to the absolute pressure, i.e. $\rho = P/RT$. The mass flow rate $M_o = A_o m_o$ through a feed orifice of discharge area $A_o = (\pi d h)$ is given by isentropic gas flow expansion formulae, and in general, a nonlinear function of the orifice to supply pressure ratio ($p = P/P_s$), i. e.

$$m(p) := \frac{P_s}{\sqrt{R \cdot T}} \cdot \begin{cases} \left(2 \cdot \frac{k}{k+1} \right)^{\frac{1}{2}} \cdot \left(\frac{2}{k+1} \right)^{\frac{1}{k-1}} & \text{if } p \leq p^{\text{r choke}} \\ \alpha \cdot \left(2 \cdot \frac{k}{k-1} \right)^{\frac{1}{2}} \cdot p^{\frac{1}{k}} \cdot \left[1 - p^{\frac{k-1}{k}} \right]^{\frac{1}{2}} & \text{if } p > p^{\text{r choke}} \end{cases} \quad \begin{cases} p^{\text{r choke}} := \left(\frac{2}{k+1} \right)^{\frac{k}{k-1}} \\ p^{\text{r choke}} = \approx 0.528 \end{cases} \quad (5)$$

Choked flow conditions are fully accounted for in the computational model. Equation (4) is solved numerically for steady-state operating conditions ($dh/dt=0$) in a fixed pad configuration. The finite difference method on discrete control volumes is used to bring equation (4) into a set of non-linear algebraic equations whose solution is sought iteratively. The algorithm of solution based on a semi-approximate analytical method introduced by Faria and San Andrés [3] is accurate even for very large surface speed conditions which effectively modifies the character of the flow from elliptical to parabolic. For this work, a grid of 80 x 20 points (circumferential x axial) defined the control volumes.

The computational program requires the bearing pad configuration and orifice distribution, pad film thickness, fluid properties, feed pressures and surface speed. Output includes the pressure field, overall mass flow rate, pad reaction forces, and orifice pressures for given orifice feed diameters, or orifice diameters for specified orifice pressures. Figure 2 shows the predicted pressure fields for the prototype configuration of the HyPad, which is a 59 degree pad with five orifices, operating at 0 rpm and 100,000 rpm, with a feed pressure three times ambient. The curves are the predicted pressure across the pad, through the orifices.

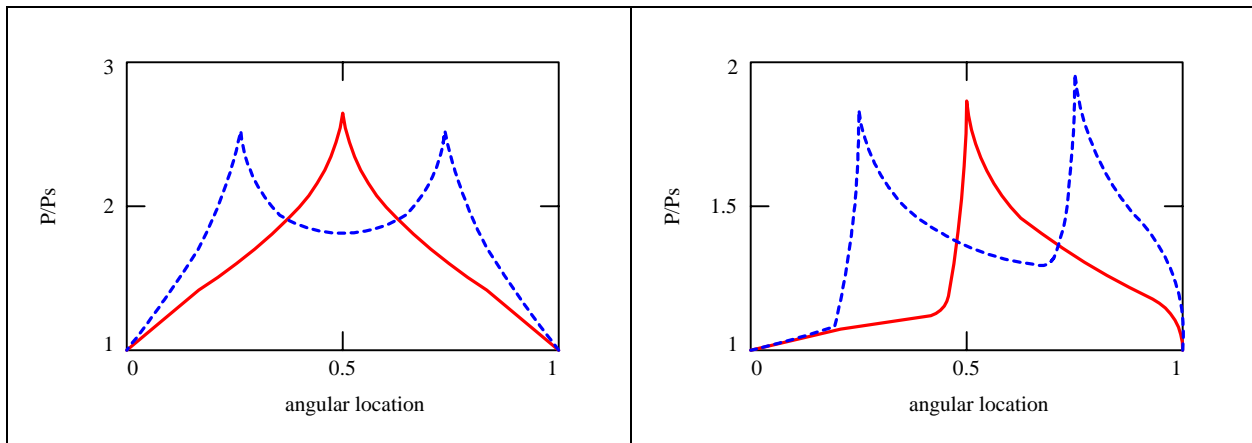


Figure 2. Pressure fields for HyPad test configuration (left - 0 rpm, right, 100,000 rpm)

In the figure, note the markedly different qualitative behavior of the pressure field for low and high rotational speeds. With no rotation, the pressure field is very symmetric, as would be expected, and develops an average pressure of approximately twice the feed pressure. At 100,000 rpm, which is the maximum speed of the rig, viscous effects skew the profile, and reduce the average pressure. Obviously, reverse injection will help this situation.

With the HyPad analysis, a plane of symmetry was used to decrease the size of the required computational grid. Pressure field output from the program for a typical 5 hole design is illustrated in Figure 3, which is a plot of the ratio of film pressure to ambient over the analysis grid, using a hydrostatic feed pressure of three times ambient. In the figure, the left hand edge is the plane of axial symmetry, thus the pressure ratios are not unity (ambient), while on the other three edges, the profile gradually decreases to ambient conditions. The pressure profile in Figure 3 shows that a fairly uniform distribution on a majority of the pad surface is obtained with the 5 hole pattern. Various off-center hole positions were considered, however, the overall profile was relatively insensitive to reasonable modifications in hole placement. Note that this analysis does not consider the angle of entrance from the outer holes, which may overstate the pressure profile.

For a single hole, the pressure dropped roughly parabolically from the center orifice. The load capacity of a single hole is up to 50% less than the 5 hole configuration, unless the orifice of the single hole is increased. For instance, the capacity of the 5 hole design in Figure 3 is 21.5 lbf, whereas the single hole design is 14.9 lbf, or 30% less even though the orifice is larger. Although a single hole configuration is not a preferred configuration, especially from a pressure distribution standpoint, the much simpler fabrication with larger orifice sizes is attractive. In the prototype testing, both five and single hole designs were evaluated.

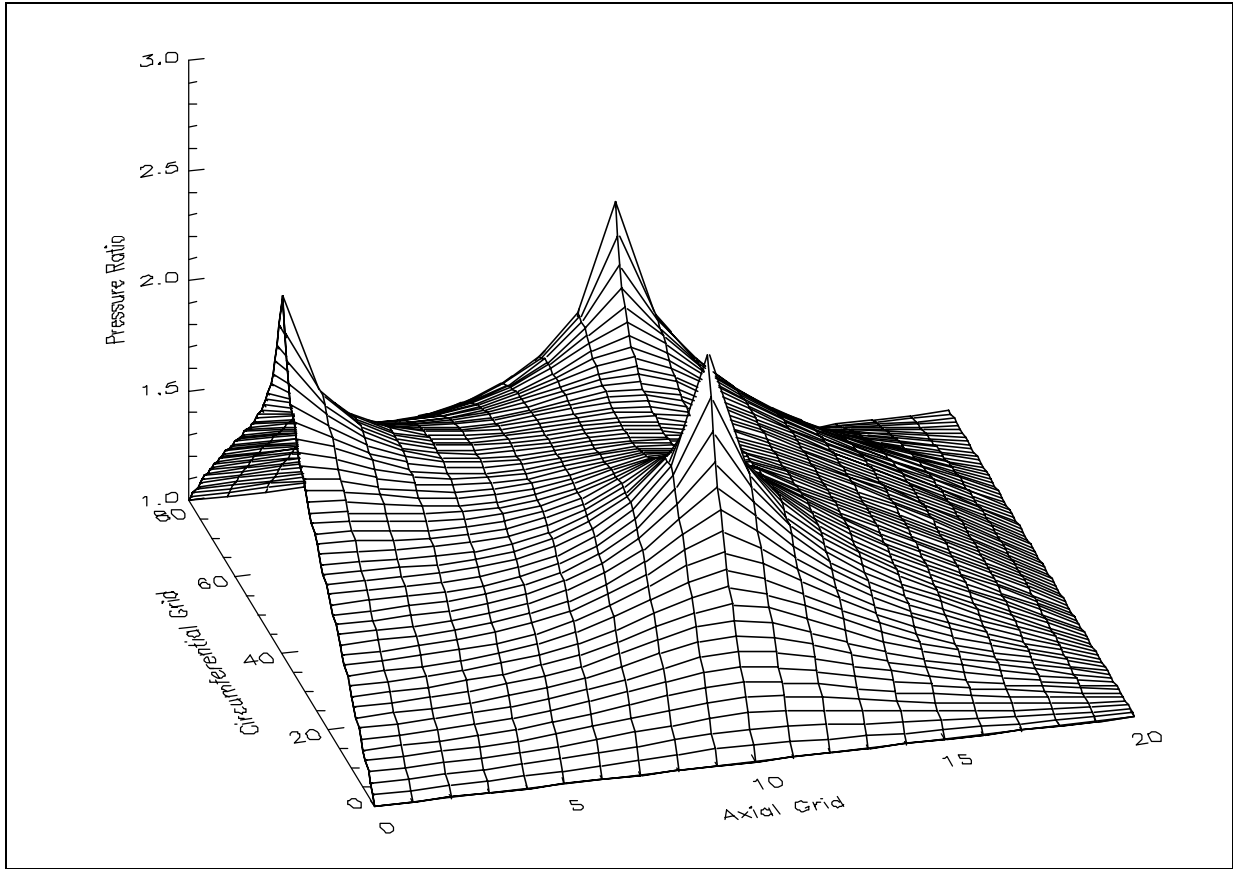


Figure 3. Pressure profile from Reynolds equation solution, 5 holes per pad

Since the Lund equations do not consider the multiple feed hole and separate pad geometry, and the Reynolds equation solver assumed no pockets, a computation fluid dynamics (CFD) analysis was used to combine both effects. A secondary benefit from the CFD analysis was an independent verification of the predictions from the Lund and Reynolds equation solutions. The CFD analysis was conducted by the Engineering Software Division of AEA Technology in El Dorado Hills, CA. Investigated in the analysis were orifice size, number of pockets, and the influence of the pockets on pressure distribution. In addition to these steady state solutions, the CFD grid was also perturbed at several different frequencies to obtain dynamic coefficients.

Typical results from the CFD analysis are illustrated in Figure 4 for the 5 hole configuration. In this case, a relatively large feed hole and pocket of 0.100 inch diameter are used, connected by a short, 0.010 inch diameter orifice. With this flow restriction, a 20 psi drop occurs across the orifice, providing the pressure compensation required for proper hydrostatic design.

A similar analysis was run for a single hole design. Comparing the results to that of the 5 hole configuration, it was observed that the regions of higher pressure cover more of the surface using 5 holes. Obviously, this implies the load capacity of the 5 hole design is larger than the single hole version, which was predicted by the Reynolds equation analysis. Conversely, the 5 holes will have more flow than a single hole, although this is somewhat balanced by the necessity to open the orifice with a single hole to have an adequate restrictor coefficient.

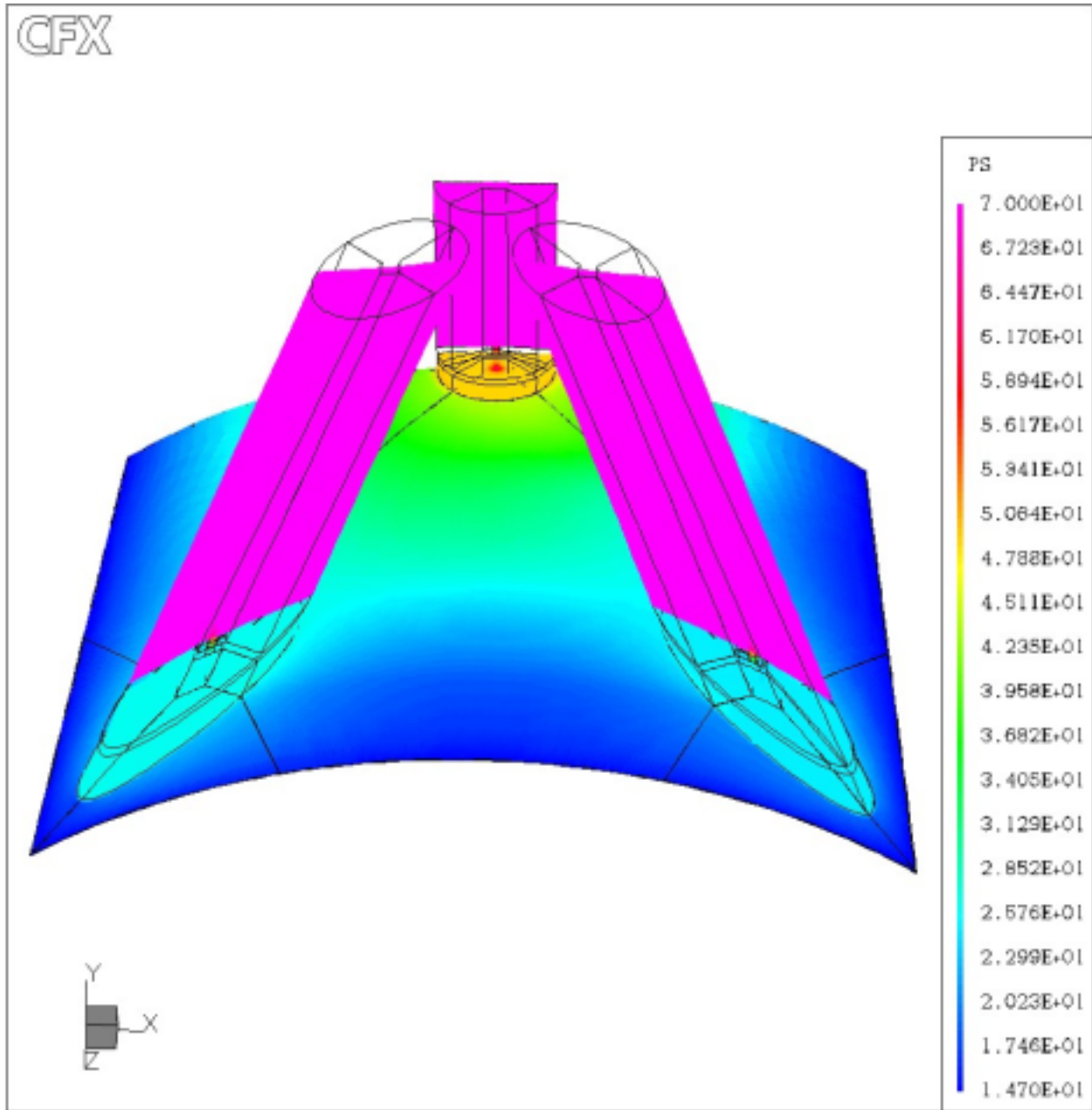


Figure 4. Pressure profile (in psi) from CFD analysis, case 2, 5 hole design

The CFD analysis also examined the exit geometry from the orifices. As noted in the discussion of the Reynolds equation solution, no pocket was included in that analysis, which is the so-called “inherently compensated” configuration. This design avoids any instability associated with pneumatic hammer, however, a rather sharp pressure drop occurs at the orifice exit, as shown with the CFD analysis, unless a recovery pocket was used. Such large pressure gradients imply losses are occurring, reducing the available pressure to support the rotor. In fact, the load capacity of the inherently compensated configuration compared to that of the 5 hole configuration with pockets was 34% less.

Based on the results of this exit analysis, some form of a pocket downstream of the orifice is necessary to assist with pressure recovery. With pneumatic hammer, this pocket volume must be kept small, as defined in the Lund analysis. Unfortunately, the CFD calculations cannot predict this type of instability, so the only method available was the Lund formulation for feed hole volume ratio. Considering available means to create small pockets, it was decided to use a drill point to create a conical volume. In all of the design configurations tested, the volume ratio V_r was consistently maintained around the recommended value defined by Lund.

Comparing the pressure profile results of the CFD analysis with that of the Reynolds equation solution, the general pressure distributions were very similar. There appears to be more edge effects in the CFD results, in that the pressure at the angled holes does not reach the center feed magnitude. This “spilling” was a concern, and the single hole pad configuration was carried in parallel, even though the load capacity and stiffness were predicted to be much less than that possible with the 5 hole design. However, the much less complicated Reynolds equation solution was adequate for design studies, although it must be enhanced to include features such as the orifice recovery pockets. For designing test hardware, the Reynolds equation solver was used to set orifice size and position, with the Lund analysis used to determine exit pocket geometry.

Design parameters for the five and single hole per pad prototype configurations are summarized in Table 1. The clearance and supply pressure (60 psig) are constant in both designs. For five holes, with an orifice of 0.010 inches, the compensation factor, feeder hole volume ratio, and restrictor coefficient are near optimum. The bearing will support 16.8 lbf, the predicted flow is roughly 0.001 lbf/sec, and the stiffness is 29,000 lbf/in. For a single hole per pad, the orifice size increases to 0.031 inches. The compensation factor is too large for maximum stiffness, because the restrictor coefficient is approaching choke. The flow is slightly less than with five holes, although the stiffness is 22,000 lbf/in, less than with the 5 hole design.

Table 1. Design parameters for HyPad prototype hardware

Parameter	5 Holes per Pad	1 Hole per Pad
Bearing Diameter, D (in)	1.1215	1.1215
Bearing Length, L (in)	1.0000	1.0000
Radial Clearance, C (in)	0.0010	0.0010
Feeder Hole Diameter, d (in)	0.040	0.040
Orifice Diameter, $2a$ (in)	0.010	0.031
Compensation Factor, δ	0.723	3.660
Restrictor Coefficient, Λ_s	0.673	0.436
Orifice Discharge Pressure, P_o (psia)	57.9	48.9
Flow rate, M_o (lbf/sec)	0.0013	0.0010
Load Capacity, F (lbf)	21.5	14.9
Stiffness, K (lbf/in)	28,600	22,300

The CFD analysis was also used to predict rotor dynamic coefficients. This was an experimental calculation obtained by transiently perturbing the analysis grid in specific directions and obtaining frequency dependent forces. Results from this approach were somewhat mixed. Predicted stiffness, based on the Lund analysis, was very similar, differing only 3%. Damping was calculated to essentially be negligible, on the order of 0.01 lbf-sec/in. Since no other means to obtain damping analytically was available, only test results could confirm or disprove this value.

TEST RESULTS

The most significant part of this project was the validation testing conducted to demonstrate the performance of the HyPad. The testing actually consisted of 2 separate parts, the first an initial feasibility demonstration, which primary sought to prove the concept worked and would operate to reasonable speeds. Subsequent testing focused on obtaining more performance data at various operating clearances and pressures.

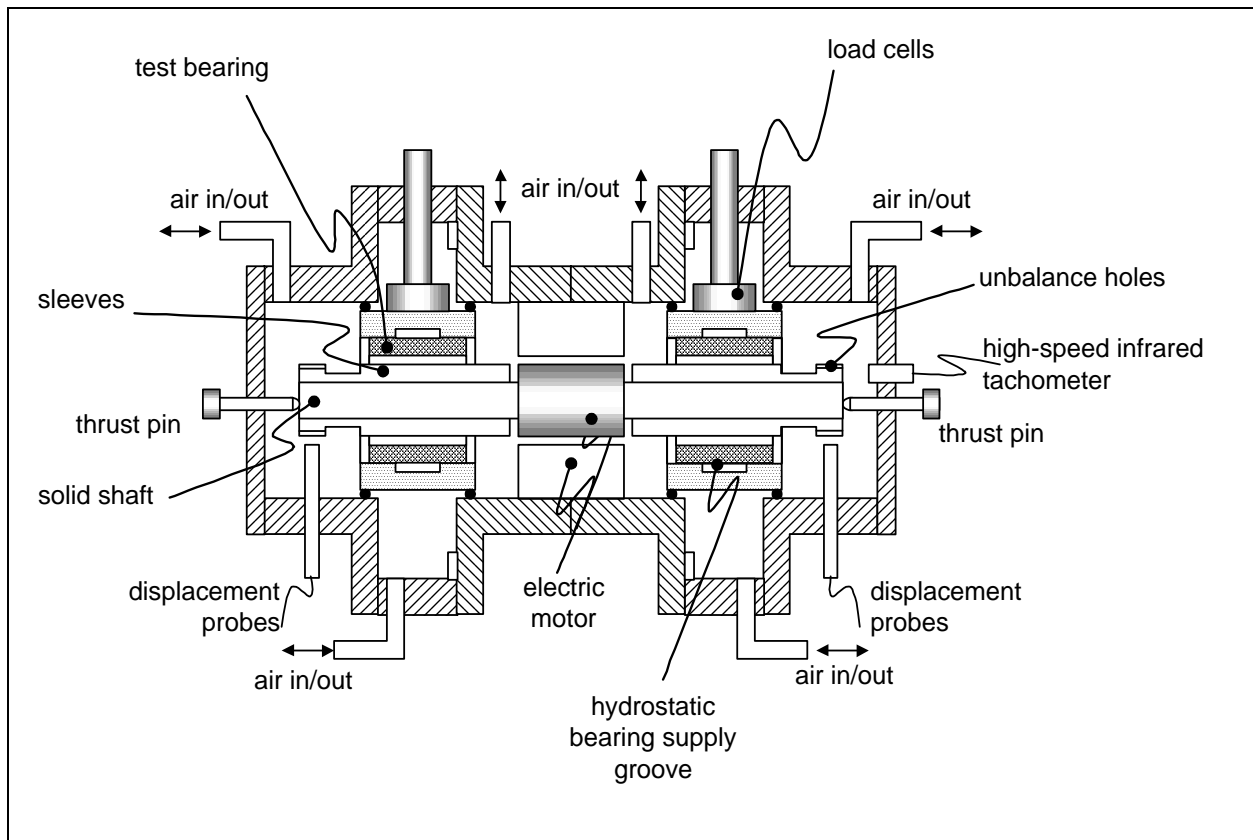


Figure 5. Texas A & M high speed gas bearing test rig

All testing was conducted using a high speed gas bearing rig at Texas A & M University. Figure 5 shows a cutaway view of the rig, in which the rotor is mounted on two cylindrical gas film bearings and supported on bearing shells attached to load cells. The rig housing has provisions for measurements of rotor displacements in two orthogonal planes and two axial positions, a number of ports for pressurized air delivery and discharge, and monitoring of temperature, pressure and rotor speed. Maximum speed of the rig is 100,000 rpm.

The rotor, weighing 1.865 lbm, consists of a solid shaft 7.48 inches long, on which an electric DC motor and two solid sleeves of 1.142 inches outer diameter are press-fitted. Three flat surfaces are machined on each bearing support, 120° apart, where three swivel-pad support bolts hold the assembly. These flats allow the use of three piezoelectric load cells to measure the forces transmitted through the bearing. Eddy current displacement sensors are installed in the vertical and horizontal directions and facing both ends of the rotor. An infrared tachometer with a maximum speed of 1,000,000 rpm is also installed on the casing.

The generic layout of the HyPad, shown in Figure 1, was refined into a test configuration that satisfied rig geometric constraints and meets acceptable design practice. The layout of this test configuration is shown in Figure 6, installed in the rig housing. Only 3 pads were used, to allow for mounting the HyPad into the rig with the load cells. The number of pads is less than what would be desired for optimum load capacity, however, sufficient enough to demonstrate and evaluate the concept. A more reasonable number of pads would be 4 or 5.

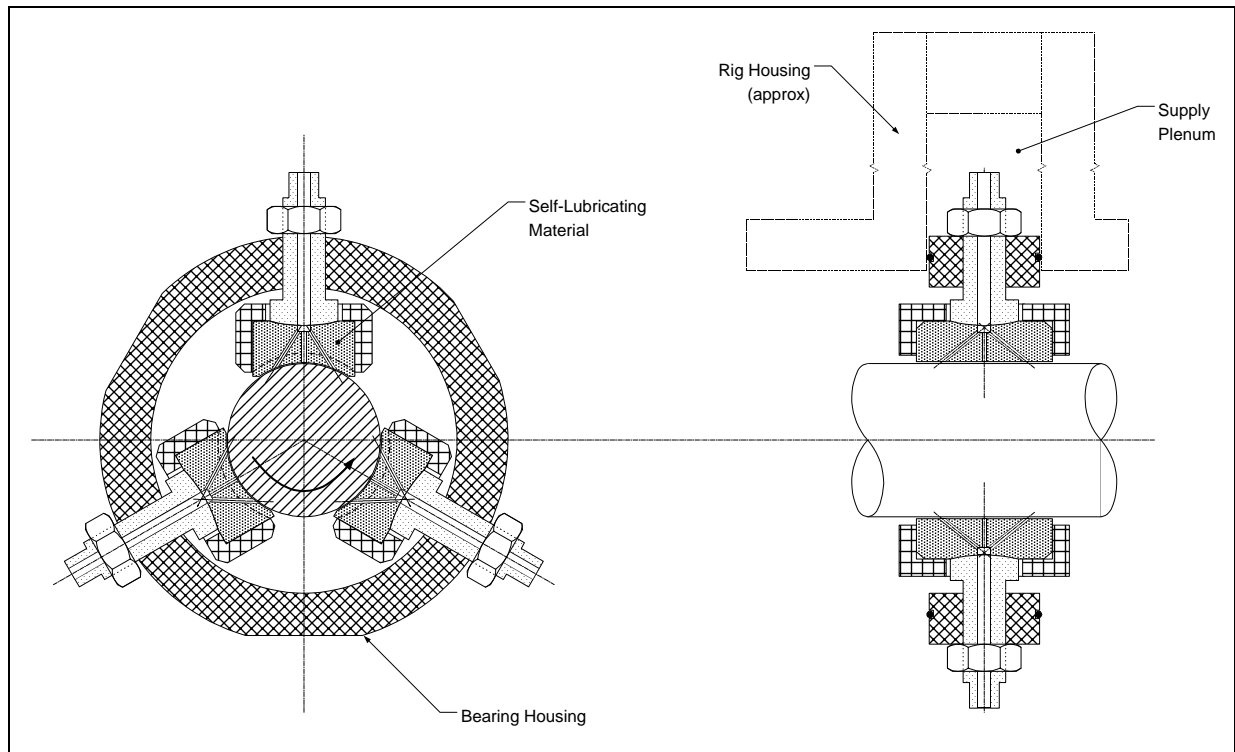


Figure 6. HyPad prototype mounted in Texas A & M test rig

The prototype HyPad bearing housing was a simple cylinder. The pad pivots were threaded into the housing, to allow for clearance control. A fine pitch thread was used to permit very small changes of radial position. A lock nut was used to fix the position once set. The actual pivot uses a very generous radius to keep the contact stresses low, limit leakage as much as possible, and reduce bending stress across the pad. The sealing scheme between the bearing mounting ring and rig housing used face seals, rather than radial O-rings, to permit a larger pad thickness and to accommodate the backing material.

Installation of the HyPad bearing into the rig was accomplished by removing the end cover and then mounting the housing ring in the 3 centering bolts, as shown in Figure 7. Before installation, the clearance of the HyPad must be set, and the center of the bearing pads must also be adjusted so that the bearing is not installed off-center. In practice, this entire procedure proved to be extremely difficult and lead to extensive manual intervention. Production configurations of the HyPad will be developed to eliminate this alignment problem.



Figure 7. Detail view of HyPad bearing installed in rig

Clearance during the initial test series using HyPad bearings at both ends of the rig was desired to be roughly 0.001 inches radial, as set with shim stock. However, the actual clearance was closer to double that amount, as determined by moving the rotor through the clearance space and watching the motion measured by the proximity probes. With the end covers installed, and when both ends were pressurized, the rotor was very free to rotate, in fact, it was found that the rotor would start spinning and reach a speed of roughly 2,800 rpm. Such levitation and rotation was very encouraging, since to operate properly, the bearing must lift the rotor off the pad surface.

Response spectra from this free rotation, with the rotor spinning at 2,800 rpm, is shown in Figure 8. Without any motor rotation, the spectra are dominated by the $\frac{1}{2}$ per rev subsynchronous whirl component at 1,400 rpm. Since the driving force behind rotation is unbalanced pressure around the circumference of the bearing, this large subsynchronous component would be expected, as bulk tangential flow is creating the torque to spin the rotor.

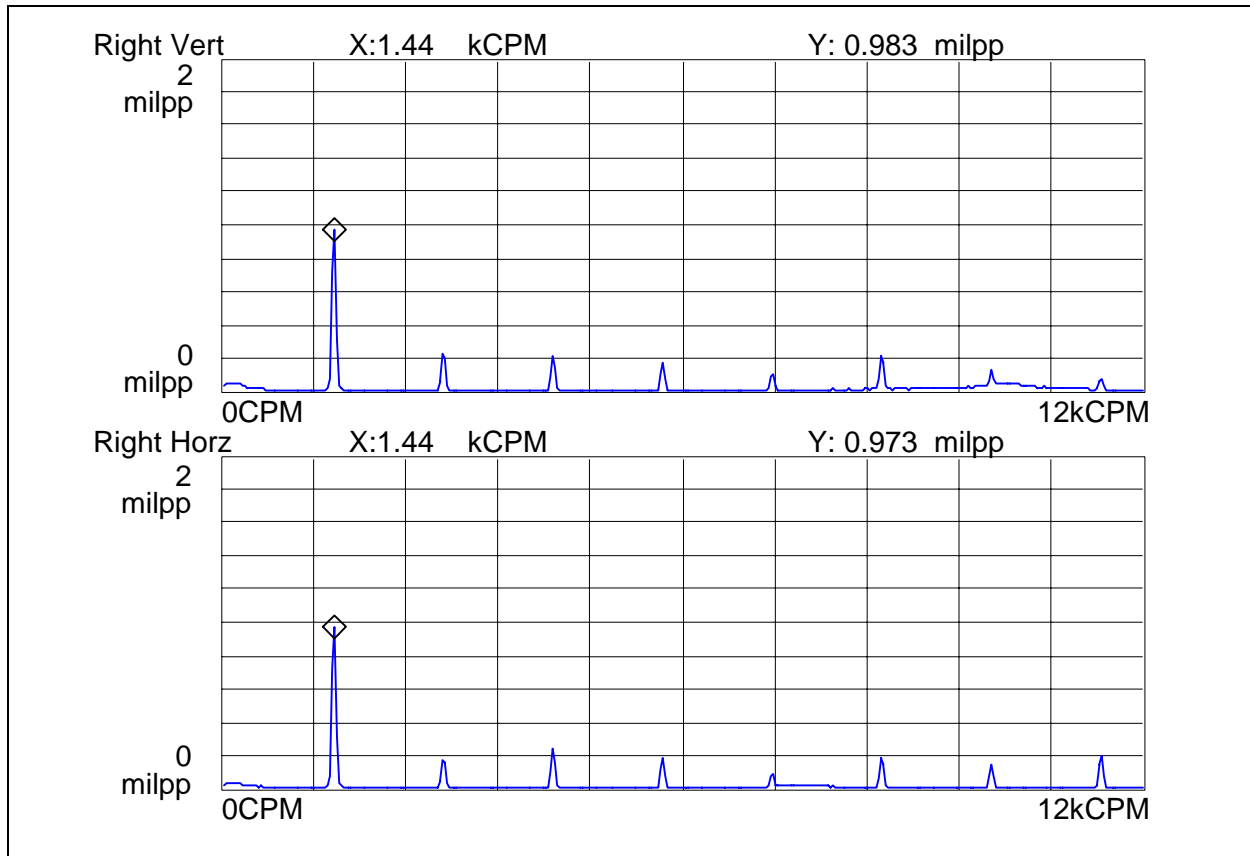


Figure 8. Response spectra of HyPad bearing freely rotating at 2,800 rpm

With the gas pressure set to maximum, which was 60 psig, the rig was gradually accelerated from the free rotation speed, carefully watching for any indication of excessive subsynchronous motion. Using fixed geometry bearings and maximum supply pressure, the rig can be run to roughly 90,000 rpm before the onset of instability occurs. When the threshold is reached, a large subsynchronous orbit is produced, and the rig must be decelerated to avoid rub damage. With the HyPad bearing, no evidence of subsynchronous vibration was observed up to 90,000 rpm! Although higher speeds could have possibly been obtained, it was not considered necessary to risk the hardware. At this speed, the HyPad was successfully supporting the rotor at a DN slightly over 2.5 million, which must be considered an outstanding demonstration of feasibility.

An example of the data obtained from the demonstration test is shown in Figure 9. This is a peak hold plot of the proximity probe data from a coastdown beginning at 90,000 rpm, with the supply pressure set at 50 psig. When the power is cut, the rig gradually slows down over a period of roughly 5 minutes. Two curves are shown, one corresponding to the vertical probe, and the other for the horizontal. In each curve, a low speed peak, at 8,600 rpm in the vertical direction and 7,200 rpm in the horizontal, are the critical speeds associated with the dynamic properties of the HyPad bearing. The different frequencies indicate the stiffness is asymmetric, which is to be expected with the 3 pad design tested. At the extreme left end of the curve, note that the mechanical runout of the rig is shown to be approximately 1.0 milpp. Since the deceleration was so gradual, the amplitude at resonance is nearly steady-state, and with a magnitude 2 – 3 times runout, the damping of the HyPad appears to be quite good, roughly 16% of critical.

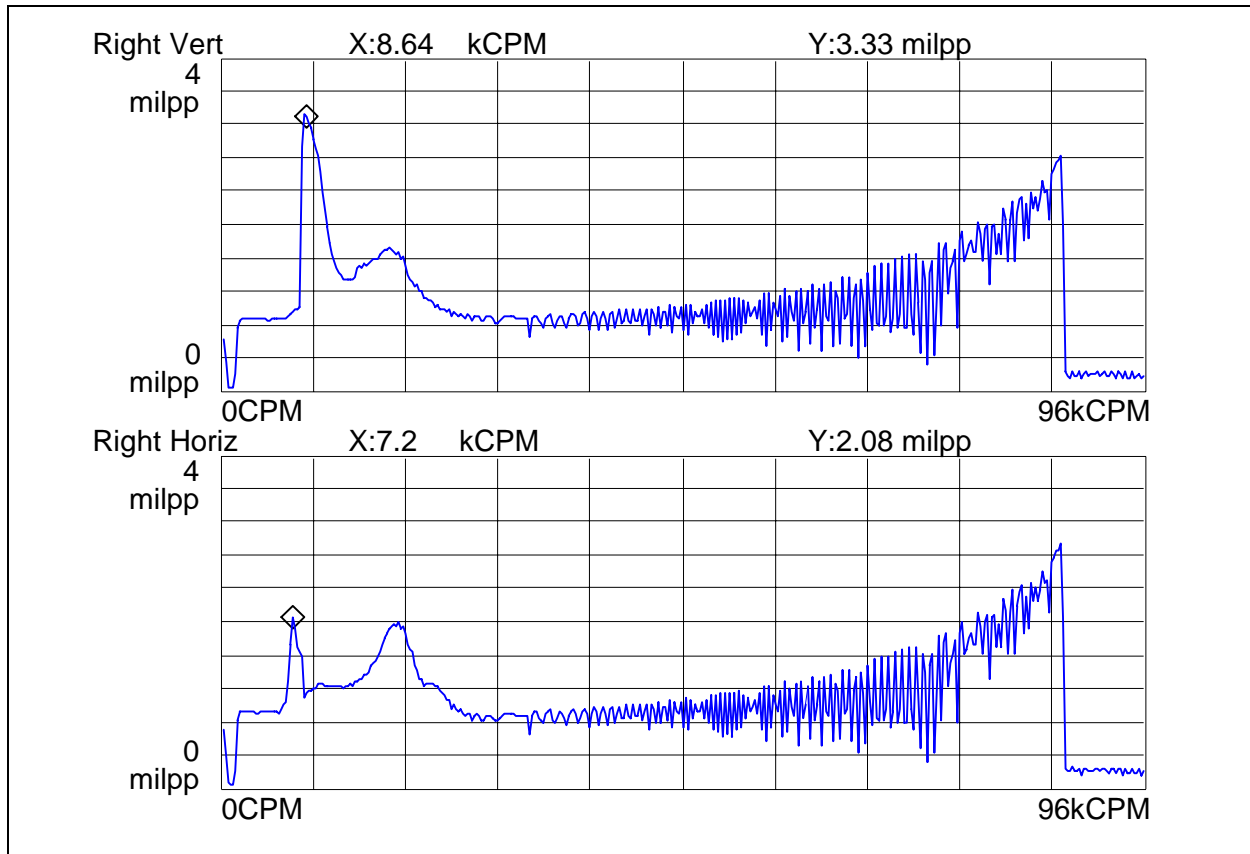


Figure 9. Coast down spectra of HyPad bearing from 90,000 rpm

The amplification factor at the low speed resonances indicates that the relatively low amount of damping predicted by the CFD analysis is not accurate. To match the resonances shown in Figure 9, using a rotor dynamics model of the rig shaft, the HyPad direct stiffness is roughly 1,800 lbf/in, with a direct damping coefficient of 0.39 lbf-sec/in. With the much larger than intended clearances, this decrease in stiffness is not surprising, however, the magnitude of damping is substantially larger than predicted from CFD, which set the coefficient at 0.01 lbf-sec/in. This discrepancy is most likely associated with the procedure used to extract the dynamic coefficients from the transient CFD results.

Above the primary resonance peaks, the response is approximately equal to the rotor runout, with a gradual climb in amplitude beginning around 60,000 rpm probably due to unbalance. The jagged spectra at the higher speeds is due to the more rapid deceleration at these frequencies contrasting with the FFT sample rate.

In terms of stability, which is a critical measure of the success of a fluid film bearing, several discrete spectra were obtained at various speeds during testing. An example of this data is shown in Figure 10, with the rig running at approximately 75,000 rpm. The only frequency component evident is at 1/rev, with a magnitude of roughly 1.700 mils pk-pk. Some amplification of motion is occurring, as the rotor is getting close to the second set of criticals. Most importantly, there essentially no subsynchronous component at $\frac{1}{2}$ per rev, unlike that observed with the free rotation. This vibration signature can be considered ideal for a bearing operating with a gas film.

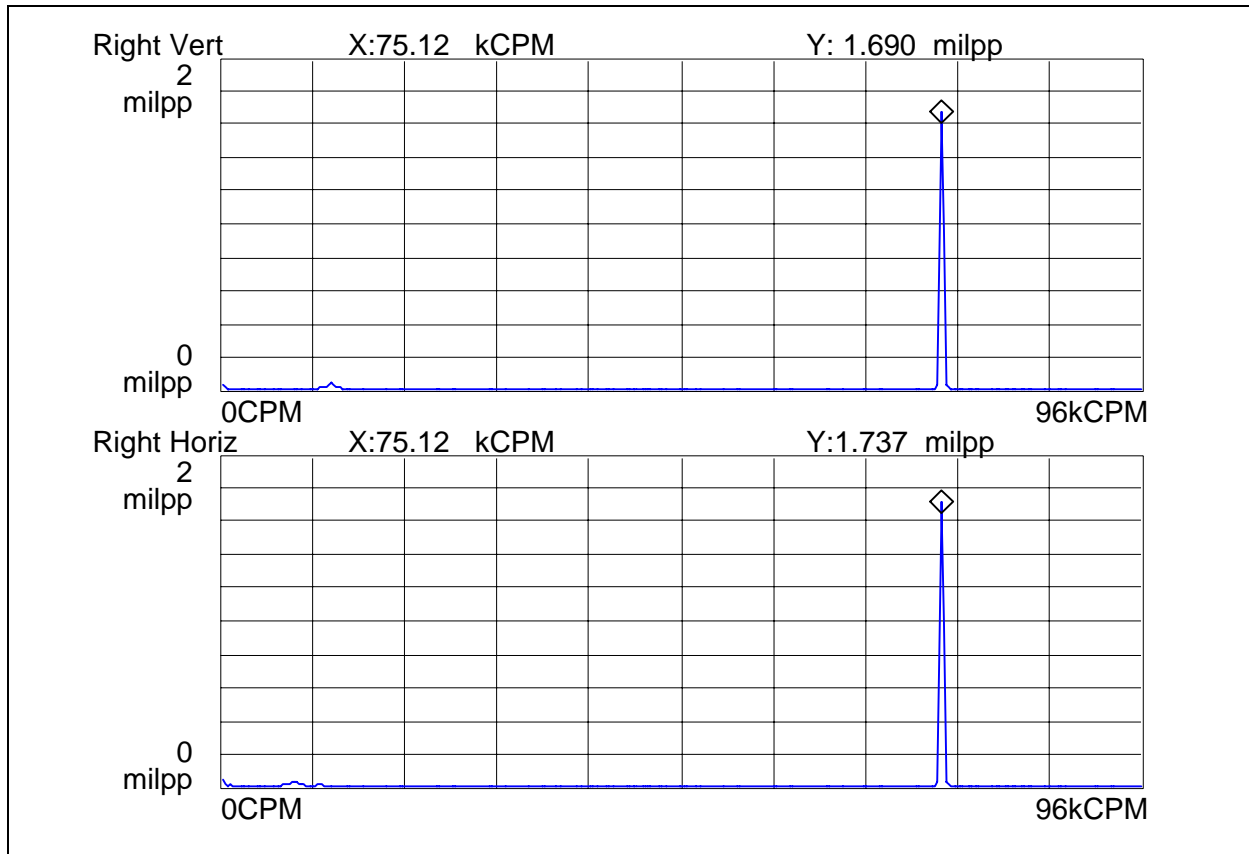


Figure 10. Vibration spectra of HyPad bearing from 75,000 rpm

The lack of subsynchronous response is not surprising. By using individual, separated pads, there is no chance for the fluid in the bearing clearance to reach a $\frac{1}{2}$ per rev bulk flow condition. In a fixed geometry bearing, viscous shear action promotes this whirl response of the gas, limiting the maximum speed achievable. With the HyPad, there should not be any practical speed limit due to bulk tangential flow.

In fact, this performance was impressively demonstrated during the testing. With the rig operating at 50,000 rpm, the supply pressure to the HyPad was gradually reduced, with very little change in response observed. Ultimately, the pressure was cut off *completely*, and the rig continued to operate normally. In essence, the HyPad was adding enough stiffness and damping through hydrodynamic action to support the rotor without instability. Note that this behavior is impossible with fixed geometry bearings alone.

Additional testing was conducted at various supply pressures and clearances to better quantify the dynamic properties of the HyPad. The rig configuration was hybrid – a fixed geometry bearing at one end and the HyPad at the other. Figure 11 depicts the vertical amplitude of synchronous rotor response recorded during coast downs from 60,000 rpm with the HyPad at 4 mils radial clearance. This large clearance was used to keep the resonances associated with the HyPad at a low speed and separate from modes due to the fixed geometry bearing.

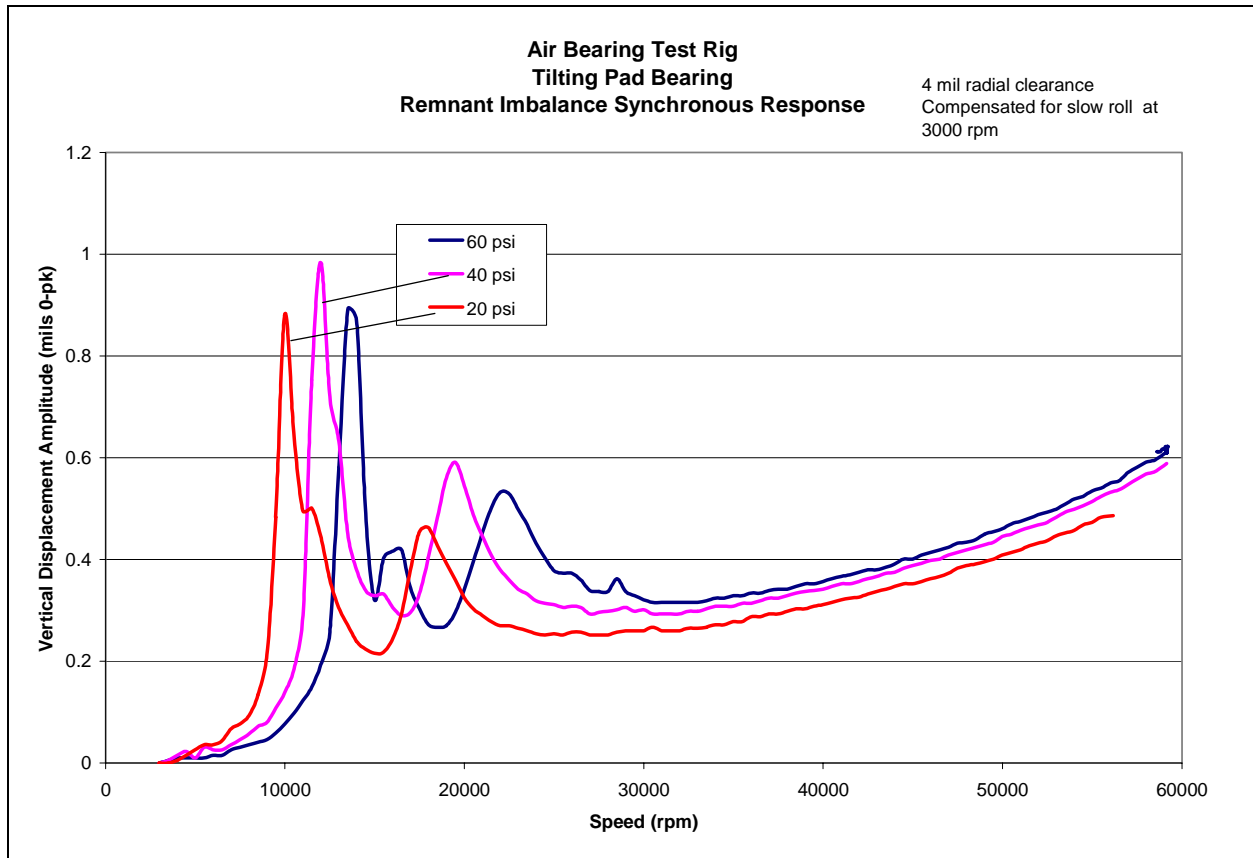


Figure 11. Rotor response to imbalance for 4 mil clearance

The results shown in Figure 11 correspond to three feed pressures equal to 20, 40 and 60 psig. For the measurements with the lowest feed pressure at the HyPad, the supply pressure into the fixed geometry bearing was 30 psig to avoid an early onset of instability. The measurements show two critical speeds that depend on the feed pressure. That is, larger feed pressures tend to stiffen the bearings increasing the critical speeds. The first critical speed ranges from 10,000 to 15,000 rpm and arises from the HyPad bearings at whose location the amplitude of vibration is roughly 1 mil with amplification factor around 3. On the other hand, the second critical speed, around 20,000 rpm, is clearly due to the fixed geometry bearing. Lower response is shown on the probes located at the HyPad end, due to the asymmetric supports.

The appearance of two distinct critical speeds follows from the dissimilar rotor dynamic coefficients (stiffness and damping) of the two bearings on which the rotor is supported. Experience with the same rotor mounted on identical bearings has shown only one critical speed around 20,000 rpm (rigid body cylindrical mode). Phase angle measurements indicate that the current critical speeds correspond to conical modes.

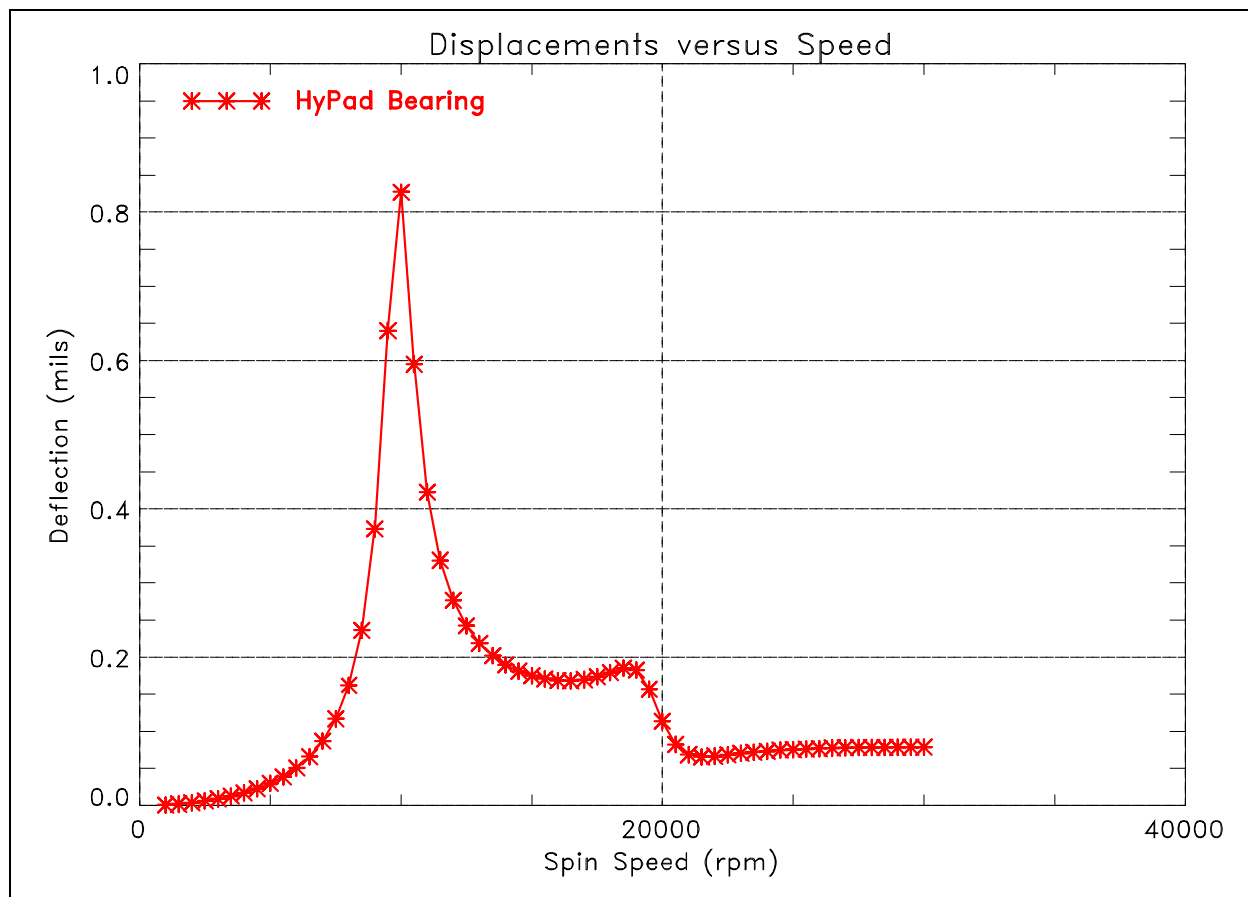


Figure 12. Calculated response to imbalance at 4 mil clearance

Data contained in Figure 11 was analytically correlated using the rotor dynamic model of the rig shaft. As displayed in Figure 12, a very good match was obtained, in this case for the response at 20 psig. Dynamic coefficients used to produce the response were a stiffness value of 2,400 lbf/in and a damping value of 0.25 lbf-sec/in or about 6% of critical. Note that the sharpness of resonance in the analytical response is very similar to the rig data, indicating the damping is well characterized. The lower damping calculated with this set of tests is to be expected, since the clearance was so large. As listed in Table 2, when the supply pressure was increased, both stiffness and damping coefficients increased as well, which is typical for hydrostatic bearings.

Table 2. HyPad dynamic coefficients at various supply pressures

Pressure (psig)	Stiffness (lbf/in)	Damping (lbf-sec/in)	Critical Damping (%)
20	2,400	0.25	5.5
40	3,200	0.25	4.9
60	4,000	0.30	5.3

(HyPad clearance = 4 mils radial)

SUMMARY AND CONCLUSIONS

This paper discussed the analysis and testing of a new concept for a gas-lubricated, oil-free bearing – the Hydrostatic Pivoted Pad or HyPad[®]. Results from the analysis and testing may be summarized as follows:

- Analysis of the flow geometry is relatively straightforward. Three different analytical procedures were used to set bearing configurations. A compressible flow Reynolds equation code was shown to produce very reliable results, as compared with a full CFD solution, for establishing size and position of the hydrostatic orifices. Exit pockets were designed based on relationships contained in a set of characterization factors taken from work by Lund. Because the gas film is created hydrostatically, between relatively rigid surfaces, the flow calculations can be greatly simplified, compared to other gas bearings such as foils.
- Testing of a prototype configuration designed with the analytical methodology produced excellent results. Using a high speed gas bearing rig, the slightly over 1 inch diameter HyPad achieved an operating speed of 90,000 rpm, equivalent to over 2.5 million DN.
- Stability of the HyPad was found to be excellent. No significant subsynchronous vibration was observed at any speed, up to the maximum attained. Another way to state this is by saying that the Whirl Frequency Ratio (cross-coupled stiffness divided by speed and damping) is very low, much less than the ½ value typical of hydrodynamic bearings. This result substantiates the use of separate pads to reduce half frequency bulk flow. In fact, the bearing was operated entirely *without* air supply, and was completely stable.
- The bearing was found to be responsive to supply pressure. As would be expected, increasing pressure increased stiffness and damping coefficients. Typical stiffness for the prototype bearing, for supply pressure up to 60 psig, was 2,000 to 4,000 lbf/in, with critical damping values from 5 to 16 percent. Much higher stiffness, and possibly damping, can be obtained with larger supply pressures.
- No evidence of pneumatic hammer was observed. This would be an obvious high frequency vibration of the pads. Careful attention to exit pocket volume was maintained with all test hardware, based on the recommendations from Lund.
- Examination of HyPad bearing surface after running did not show any evidence of significant wear. Of course, the operating time was very limited, however, numerous starts and stops were performed, and a great deal of manual rotation was applied while trying to align the bearing in the rig.

The results from the testing provide convincing evidence that the HyPad concept has great promise. Coupled with the relatively simple analytical methods needed to design the flow geometry, the HyPad is a good candidate for replacing conventional oil-lubricated rolling element bearings in small gas turbine engines.

ACKNOWLEDGEMENTS

Work on this project was conducted under a Small Business Innovation Research contract through the Air Force Research Laboratory, with Matthew Wagner as the technical monitor, whose support is gratefully acknowledged. The assistance from Prof. Luis San Andrés and Deborah Wilde of Texas A & M during testing is also greatly appreciated.

REFERENCES

1. Agrawal, Giri L., "Foil Air/Gas Bearing Technology ~ An Overview," ASME Paper 97-GT-347, (1997).
2. Lund, Jorgen W., "Gas Bearing Design Charts, Volume 2, Hydrostatic Gas Journal and Thrust Bearing," Mechanical Technology Report MTI-65TR5-II, April 1, 1965.
3. Faria, M., and L. San Andrés, "On the Numerical Modeling of High Speed Hydrodynamic Gas Bearings," ASME Journal of Tribology, Vol. 122, 1, pp. 124-130, 2000 (ASME Paper 99-TRIB-2).

NOMENCLATURE

As referenced in the text of this paper, Table 3 lists the nomenclature used to describe various physical quantities associated with the design and analysis of the HyPad bearing.

Table 3. List of nomenclature

Symbol	Description	Symbol	Description
a	Flow Orifice Radius	P_a	Ambient Pressure
C	Radial Clearance	P_o	Orifice Discharge Pressure
d	Feeder (Exit) Hole Diameter	P_s	Supply Pressure
D	Bearing Diameter	R	Gas Constant
F	Load Capacity	T	Gas Temperature
h	Film Thickness	U	Rotor Surface Speed
K	Direct Stiffness	V_c	Exit Hole (Pocket) Volume
L	Bearing Length	V_r	Feeder Hole Volume Ratio
m_o	mass flow per unit area	δ	Inherent Compensation Factor
M_o	Mass Flow Rate	Λ_s	Restrictor Coefficient
N	Number of Feed Holes	μ	Gas Viscosity
P	Fluid Pressure	ρ	Fluid Density